PAPER • OPEN ACCESS

Terahertz quantum-cascade lasers for high-resolution absorption spectroscopy of atoms and ions in plasmas

View the article online for updates and enhancements.

You may also like

Terahertz quantum-cascade lasers for high-resolution absorption spectroscopy of atoms and ions in plasmas

X Lü[1,*] ![ORCID], B Röben[1,3] ![ORCID], K Biermann[1] ![ORCID], J R Wubs[2] ![ORCID], U Macherius[2], K-D Weltmann[2] ![ORCID], J H van Helden[2] ![ORCID], L Schrottke[1] ![ORCID] and H T Grahn[1] ![ORCID]

[1] Paul-Drude-Institut für Festkörperelektronik, Leibniz-Institut im Forschungsverbund Berlin e. V., Hausvogteiplatz 5–7, 10117 Berlin, Germany
[2] Leibniz Institute for Plasma Science and Technology (INP), Felix-Hausdorff-Str. 2, 17489 Greifswald, Germany

E-mail: lue@pdi-berlin.de

CrossMark

Abstract
We report on terahertz (THz) quantum-cascade lasers (QCLs) based on GaAs/AlAs heterostructures, which exhibit single-mode emission at 3.360, 3.921, and 4.745 THz. These frequencies are in close correspondence to fine-structure transitions of Al atoms, N^+ ions, and O atoms, respectively. Due to the low electrical pump power of these THz QCLs, they can be operated in a mechanical cryocooler in continuous-wave mode, while a sufficient intrinsic tuning range of more than 5 GHz is maintained. The single-mode operation and the intrinsic tuning range of these THz QCLs allow for the application of these lasers as radiation sources for high-resolution absorption spectroscopy to determine the absolute densities of Al atoms, N^+ ions, and O atoms in plasmas.

Keywords: terahertz quantum-cascade lasers, emission frequency, GaAs/AlAs

(Some figures may appear in colour only in the online journal)

1. Introduction

Quantum-cascade lasers (QCLs) are excellent sources for high-resolution spectroscopy in the terahertz (THz) spectral region [1–8]. Presently, compact sources emitting at 3.360, 3.551, 3.921, and 4.745 THz are of particular interest in astronomy and plasma science for the detection and investigation of aluminum atoms [9], hydroxyl radicals [10], nitrogen ions [11], and oxygen atoms [12], respectively. For example, the $^1F_{5/2} \leftarrow {}^1F_{7/2}$ rotational transition of the hydroxyl radical at 3.5512 THz and the $^3P_1 \leftarrow {}^3P_2$ fine-structure transition of neutral atomic oxygen at 4.7448 THz play an important role in the research of the Earth's atmosphere [13–15]. In addition, atomic oxygen also exists in interstellar media. For atmospheric research and astronomy, heterodyne spectrometers are usually employed [16], while absorption spectroscopy is used in plasma science [17, 18]. For both applications, the QCLs have to be operated in continuous-wave (cw) mode exhibiting a single mode with an output power of at least 1 mW at the target frequency. Furthermore, the QCLs should exhibit an intrinsic tuning range of at least

5 GHz. Since THz QCLs have to be operated under cryogenic conditions and their output power decreases with increasing operating temperature, a practical operating temperature T_{po} is defined as the highest operating temperature with an output power of at least 1 mW [19]. According to the cooling capacity of typical coolant-free systems at temperatures between 50 and 60 K, an electrical pump power P_{pump} (the product of the driving current and the voltage) of less than a few watts is required for practical applications. At the same time, the realization of a QCL emitting at a specific target frequency is challenging, since the gain maxima have to be sufficiently close to the target frequencies and the laser bars have to be precisely cleaved to the correct length in order to achieve the exact frequencies.

Up to now, astrophysical applications using THz QCLs mainly focus on the local oscillator at 4.745 THz. There are two strategies to realize QCLs emitting at 4.745 THz. In strategy I, the active region is based on a relatively straightforward resonant-phonon design [20], but the laser cavity requires sophisticated engineering using metal–metal waveguides, lateral distributed-feedback gratings, and antenna coupling. Kloosterman *et al* [21] reported a local oscillator at 4.741 THz using a third-order distributed-feedback QCL. At 10 K, the cw output power was 0.25 mW using $P_{pump} \approx 0.7$ W. At 77 K, the tuning range was 3 GHz. Bosco *et al* [22] reported on a 4.745 THz QCL using a patch-array antenna together with a first-order lateral distributed-feedback grating. At 10 K, the cw output power amounted to 1.0 mW using $P_{pump} \approx 1.6$ W with a 3 GHz tuning range. Khalatpour *et al* [23, 24] reported on an array of 18 unidirectional antenna-coupled third-order distributed-feedback QCLs for the local oscillator at 4.745 THz of the *Galactic/Extra Ultra-Long-Duration Balloon Spectroscopic-Stratospheric Terahertz Observatory* (GUSTO), which is based on a unidirectional wire laser. At 55 K, the cw output power of one QCL in the array amounted to more than 8 mW using $P_{pump} \approx 2.2$ W with a 6 GHz tuning range. In strategy II, Fabry–Pérot resonators based on surface-plasmon waveguides are employed, while a rather sophisticated hybrid design is used for the active region, which combines the advantages of the bound-to-continuum design and the resonant-phonon design [25, 26]. Based on this strategy, 4.745 THz QCLs have been developed, which have been used in the local oscillator for the *German REceiver for Astronomy at Terahertz frequencies* (GREAT) heterodyne spectrometer on the *Stratospheric Observatory for Infrared Astronomy* (SOFIA) [27]. In one of the earlier missions, for example, atomic oxygen was detected in the thermosphere of Mars [28, 29]. A recent, compact THz source based on a 4.745 THz QCL provided up to 8 mW output power with $P_{pump} < 1.8$ W [30]. At 60 K, the tuning range covers the frequency range from −0.7 to +3.8 GHz with respect to the atomic oxygen transition at 4.7448 THz.

For plasma science, the density of the atoms and ions of interest is determined by evaluating the spectral profiles of the respective high-resolution absorption features. In this configuration, the QCLs have to fulfill similar operating parameters as for the local oscillators in heterodyne spectrometers: (a) the lasers have to exhibit single-mode emission at a frequency matching the transition frequency with a precision of several GHz and a sufficient tuning range in order to cover the complete absorption profile. (b) The output power has to reach values of about 1 mW. (c) The pump power has to be located in the range between 1 and 2 W. Therefore, the strategy for the development of the lasers is very similar to the approach for the local oscillators. Furthermore, the lasers have to allow for a continuous frequency tuning, which is achieved by a fast ramping of the injection current without abrupt changes. Therefore, instabilities such as mode jumping and discontinuous changes of the output power have to be avoided for the entire tuning range. Such a stable operation in the fast-ramping mode is an additional challenge for the development of THz QCLs for high-resolution spectroscopy.

For the development of lasers for absorption spectrometers, we focus on strategy II. In a first step, we choose a heterostructure design which exhibits its gain maximum close to the target frequency. Then, we select an appropriate piece of the wafer based on the method described in [31], since the emission frequency is a function of the position on the wafer. As indicated in [32], the exact value of the frequency of a laser mode in a Fabry–Pérot resonator depends sensitively on the exact length of the resonator, which imposes a challenge for cleaving a laser bar. A frequency precision of 1 GHz corresponds to a length precision of about 1 μm. An alternative method to reach the exact frequency is to precisely adjust the resonator length after cleavage by polishing the facets [32].

In the present study, we realize, in addition to a single-mode QCL for detecting O atoms at 4.7448 THz with a tuning range of several GHz and an output power of 1 mW, two single-mode QCLs for detecting Al atoms and N^+ ions at 3.3596 and 3.9205 THz, respectively, with sufficiently large tuning ranges and output powers. We determined the operating parameters such as emission frequency, output power, tuning range, P_{pump}, and T_{po} for several sets of lasers and then selected appropriate THz QCLs to be used in a high-resolution absorption spectrometer for the detection of the Al atoms, N^+ ions, and O atoms.

2. Design, materials system, and resonator

For high-temperature cw operation, THz QCLs based on the so-called hybrid design have been found to be advantageous. This design combines low-voltage operation of bound-to-continuum designs with high output powers of resonant-phonon designs. The majority of THz QCLs relies on GaAs/(Al, Ga)As heterostructures. For the hybrid design, we were able to develop lasers with three times larger wall plug efficiencies in comparison to their (Al, Ga)As counterparts using nominally binary AlAs barriers [33]. Fabry–Pérot resonators with surface plasmon waveguides are a straightforward approach for applications, since they allow for a rather large light out-coupling and for a larger yield of devices per wafer area. For lasers with sufficient gain, single-mode operation can be realized for short Fabry–Pérot resonators, for which the mode spacing is larger than the width of the gain spectrum. For

GaAs/AlAs THz QCLs emitting at 3.5 and 4.7 THz, a practical operating temperature above 75 K has already been demonstrated [30].

3. Experimental details

The GaAs/AlAs THz QCLs were grown on 2 inch wafers in a molecular beam epitaxy system (VG 8-port V80H) with an average growth rate of $0.13\,\mathrm{nm\,s^{-1}}$. The fluctuations in the growth rates are below 1% due to the use of a closed-loop rate control system based on optical reflection measurements for the *in-situ* growth control [34]. The lasers are based on single-plasmon waveguides and processed by photolithography and standard wet chemical etching. The lasers are operated in a Stirling cryocooler (Ricor K535). The lasing spectra are measured using a Fourier-transform infrared spectrometer Bruker IFS 120/5 HR with a resolution of $0.07\,\mathrm{cm^{-1}}$ (2.1 GHz). The optical power of all lasers was determined using a power meter (SLT THz 20), which was calibrated in the THz spectral range by the German National Metrology Institute (Physikalisch-Technische Bundesanstalt). For the measurement of the emission spectra at a particular operating temperature, a temperature monitoring program is applied to maintain a stable temperature of the heat sink during the measurement.

4. Lasers for the detection of Al, N$^+$, and O in plasmas

Starting point for the design of the lasers was the 4.745 THz GaAs/(Al,Ga)As QCL used in the local oscillator for the GREAT heterodyne spectrometer on SOFIA [28], the design of which was subsequently transferred to the GaAs/AlAs materials system [33]. GaAs/AlAs QCLs for the Al and N$^+$ absorption lines have been obtained by a scaling of the design parameters of the 4.745 THz QCL, including the necessary adjustment of several layer thicknesses [19]. In order to select lasers with gain maxima at the respective target frequencies, we made use of the lateral grading of the layer thicknesses and hence the frequency of the gain maximum. Due to a lateral inhomogeneity of the growth rate, the period length of the QCLs decreases from the center to the edge of the wafer, which results in a blue shift of the gain maximum. Based on the method described in [31], we identified three wafers for which the expected frequency ranges of the gain medium include the frequencies 3.360, 3.921, and 4.745 THz. By using the correlation between the frequency and the distance R from the center of the wafer [31], we determined the location, where a QCL with a suitable length is expected to emit at the target frequency. On the three wafers for 3.360, 3.921, and 4.745 THz, we found appropriate pieces at $R \approx 8$, 3, and 12 mm, respectively. In the range of $(R \pm 1)$ mm, we mounted two or three QCLs with different lengths and measured the light output-current density-voltage (L–J–V) characteristics as well as the lasing spectra. For example, for 3.921 THz, we investigated two QCLs with cavity lengths of about 0.7 and 0.8 mm in the range of $R = 2$ to 4 mm. We found one of them operating in
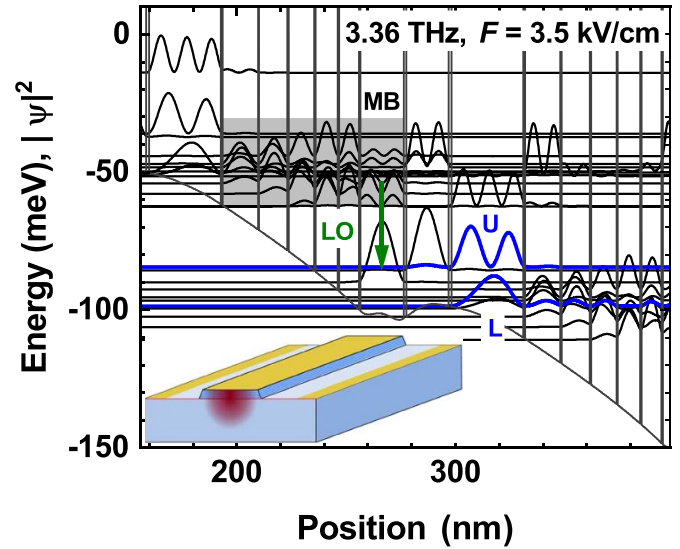

Figure 1. Conduction band profile and subband structure of QCL A for 3.360 THz. The inset shows an illustration of the single-plasmon waveguide. The upper and lower laser levels are marked as U and L, respectively. MB denotes the quasi-miniband, and LO depicts the transition resonant to the longitudinal optical phonon. The carriers can be extracted efficiently from MB into the injector level by longitudinal-optical-phonon scattering.

single mode emitting at 3.921 THz with a tuning range of more than 6 GHz and an output power of up to 2 mW. At the same time, this laser satisfies the requirements for stable frequency tuning, i.e. neither mode jumps nor discontinuities in the output power are observed over the entire tuning range. Based on this method, we obtained QCLs for all frequencies with tuning ranges of several GHz. We label these lasers as A (3.360 THz), B (3.921 THz), and C (4.745 THz).

Figure 1 depicts the subband structure of QCL A as well as an illustration of the single-plasmon waveguide. The details of the design of samples A, B, and C are given in[4], [5], and[6], respectively. As we pointed out in section 1, we apply strategy II to realize a QCL emitting at a specific frequency, which employs Fabry–Pérot resonators with surface plasmon waveguides. We found that we need to mount less than ten lasers to achieve the required operating parameters. In comparison to strategy I, which uses engineered cavities, the advantage

[4] QCL A corresponds to sample PDI-M4-3478. The nominal layer sequence starting from the injection barrier is **1.12**, 33.1, **0.56**, 16.3, **0.42**, 13.1, **0.42**, 11.7, **0.42**, 10.5, **0.42**, 9.3, **0.42**, <u>20.0</u>, **0.84**, 19.6 with the layer thicknesses in nm. Bold numbers denote the AlAs barriers, while the underlined number indicates the doped layer. The nominal doping density is $2.0 \times 10^{17}\,\mathrm{cm^{-3}}$.

[5] QCL B corresponds to sample PDI-M4-3440. The nominal layer sequence starting from the injection barrier is **1.12**, 29.9, **0.56**, 16.1, **0.42**, 12.8, **0.42**, 11.3, **0.42**, 9.6, **0.42**, 8.8, **0.42**, <u>19.1</u>, **0.96**, 19.1 with the layer thicknesses in nm. Bold numbers denote the AlAs barriers, while the underlined number indicates the doped layer. The nominal doping density is $2.0 \times 10^{17}\,\mathrm{cm^{-3}}$.

[6] QCL C corresponds to sample PDI-M4-3146. The nominal layer sequence starting from the injection barrier is **1.12**, 27.2, **0.56**, 15.0, **0.42**, 12.1, **0.42**, 10.8, **0.42**, 9.2, **0.42**, 8.1, **0.28**, 2.0, **0.28**, <u>17.7</u>, **1.12**, 15.7 with the layer thicknesses in nm. Bold numbers denote the AlAs barriers, while the underlined number indicates the doped layer. The nominal doping density is $3.0 \times 10^{17}\,\mathrm{cm^{-3}}$.

Table 1. Operating parameters for QCLs A, B, and C. ν_{mode} denotes the frequency range of the observed lasing modes, T_{po} the practical operating temperature, T_{hs} the heat sink temperature, $\Delta\nu$ the intrinsic tuning range, L the output power, and J_{th} the threshold current density. The values for $\Delta\nu$, L, and J_{th} have been determined at T_{hs} of 45 K for QCLs A as well as C and of 40 K for QCL B.

QCL	ν_{mode} (THz)	T_{po} (K)	T_{hs} (K)	$\Delta\nu$ (GHz)	L (mW)	J_{th} (A cm^{-2})
A	3.358–3.364	67	45	3.4	3.2	188
B	3.912–3.923	60	40	6.9	2.1	215
C	4.738–4.748	59	45	3.7	7.9	335

of strategy II is the relatively simple fabrication of the cavity. At the same time, less material is consumed. When a replacement QCL emitting at the same target frequency is required, we will probably find one in the range with similar values of R on the wafer. On the one hand, the lateral inhomogeneity of the wafers allows us to compensate for the limited growth reproducibility so that only a few wafers have to be grown to obtain a number of QCLs emitting at the target frequency. On the other hand, the yield of useable lasers from one wafer is reduced. However, an improvement of the growth reproducibility for the GaAs/AlAs THz QCLs based on the complex hybrid design is still rather challenging. With a better reproducibility, the total yield of suitable lasers may be increased by an improved lateral homogeneity, which can be achieved by an appropriate modification of the geometry of the growth chamber. In table 1, we present the total frequency ranges of the observed lasing modes by tuning the driving current and the heat sink temperature T_{hs}, the practical operating temperatures, and, for a particular value of T_{hs} (40 or 45 K), the intrinsic tuning ranges, the output powers, as well as the threshold current densities for QCLs A, B, and C.

Figure 2 shows the L–J–V characteristics as well as the emission spectra of QCL A for the detection of Al atoms (transition at 3.3596 THz) under various operating conditions. As indicated in [31], P_{pump} is also an important operating parameter for cw operation. To maintain a stable temperature of the heat sink, P_{pump} of a QCL has to be lower than the cooling capacity of the Stirling cryocooler, which has an impact on the dynamic range of the lasing for current as well as temperature tuning. At 35 K, the maximum electrical pump power of QCL A is about 1 W, which is clearly below the cooling capacity of the cryocooler (1.2 W). Thus, the laser can be stably operated over a wide range of applied-current values, and the corresponding current tuning range is 3.8 GHz. At 35 K, an output power of about 3.5 mW is achieved. At a temperature above 35 K, the increasing cooling capacity of the cryocooler, e.g. 2.8 W at 45 K, makes cw operation possible for the whole dynamic range. For heat sink temperatures up to 60 K, QCL A emits always in a single mode as shown in figure 2(b). Note that due to the instrument function, the linewidth of the measured spectra is much wider than the laser linewidth, which is about several MHz for a free-running QCL. The lasing frequency in this regime can be tuned between 3.358 and 3.364 THz, which includes the frequency of the transition of Al atoms. This tuning range of 5.4 GHz is sufficient for high-resolution spectroscopy
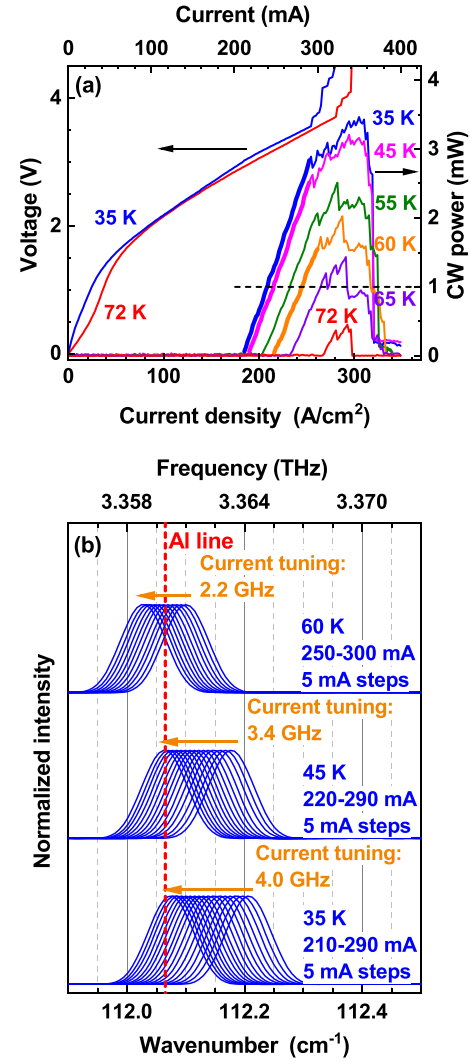

Figure 2. (a) L–J–V characteristics for several operating temperatures and (b) lasing spectra for several operating temperatures and current densities of QCL A under cw operation with laser ridge dimensions of 0.12×0.96 mm^2. The thick solid lines of the L–J curves in (a) show the range of the current corresponding to the spectra in (b). The dashed line in (a) indicates the power of 1 mW as a guide to the eye. The dashed line in (b) indicates the target frequency of 3.3596 THz (Al transition).

of low-pressure absorption features. The value for T_{po} is currently 67 K.

Figure 3 shows the L–J–V characteristics as well as the emission spectra of QCL B for the detection of N$^+$ ions (transition at 3.9205 THz) under various operating conditions. At 35 K, the values of the threshold current density J_{th} and the maximum pump power $P_{pump,max}$ of QCL B are 204 A cm^{-2} and 1.7 W, respectively, which are larger than the corresponding values for QCL A (181 A cm^{-2} and 1.0 W). Note that the current dynamic range of QCL B (204–424 A cm^{-2}) is obviously larger than that of QCL A (181–254 A cm^{-2}), which results in a current tuning range of more than 6 GHz for QCL B. $P_{pump,max}$ amounts to 1.6 W at 40 K for QCL B, which is smaller than the cooling capacity of the cryocooler (2 W) so that the laser can be stably operated over the whole dynamic range.
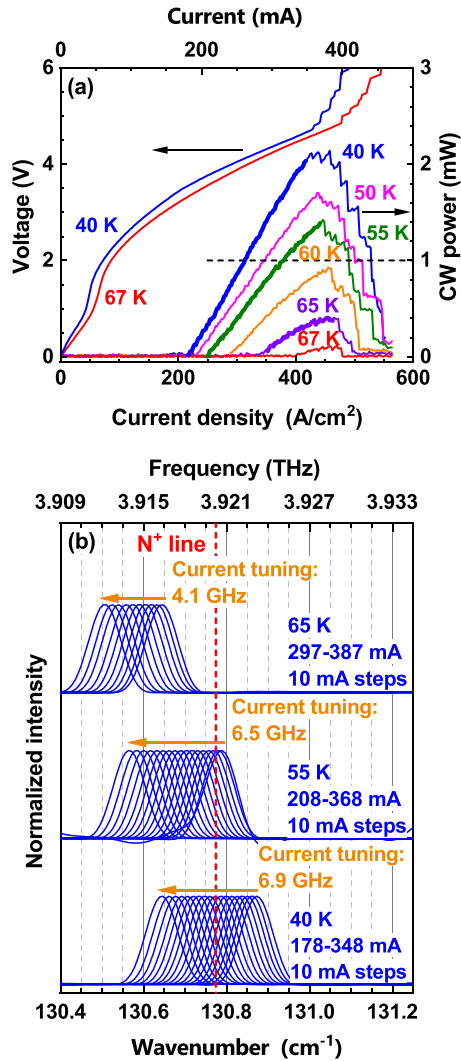
Figure 3. (a) *L–J–V* characteristics for several operating temperatures and (b) lasing spectra for several operating temperatures and current densities of QCL B under cw operation with laser ridge dimensions of $0.12 \times 0.70\,\mathrm{mm}^2$. The thick solid lines of the *L–J* curves in (a) show the range of the current corresponding to the spectra in (b). The dashed line in (a) indicates the power of 1 mW as a guide to the eye. The dashed line in (b) indicates the target frequency of 3.9205 THz (N^+ transition).
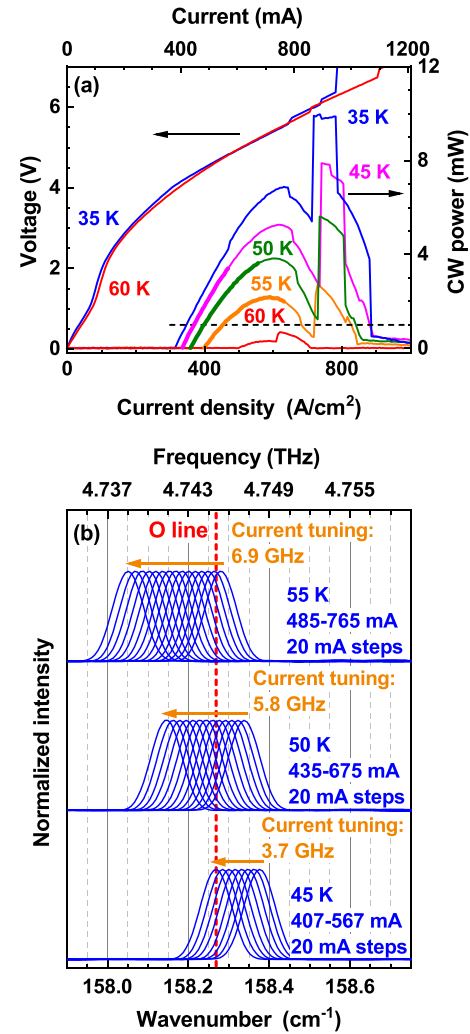
Figure 4. (a) *L–J–V* characteristics for several operating temperatures and (b) lasing spectra for several operating temperatures and current densities of QCL C under cw operation with laser ridge dimensions of $0.12 \times 1.01\,\mathrm{mm}^2$. The thick solid lines of the *L–J* curves in (a) show the range of the current corresponding to the spectra in (b). The dashed line in (a) indicates the power of 1 mW as a guide to the eye. The dashed line in (b) indicates the target frequency of 4.7448 THz (O transition).

The corresponding current tuning range is 6.9 GHz. For temperatures up to 60 K, QCL B emits always in a single mode, and an output power larger than 1.0 mW is achieved as shown in figure 3. The lasing frequency in this regime can be tuned between 3.912 and 3.923 THz, which includes the frequency of the transition of N^+ atoms (3.9205 THz).

Figure 4 shows the *L–J–V* characteristics as well as the emission spectra of QCL C for the detection of O atoms (transition at 4.7448 THz) under various operating conditions. By neglecting the complex structures for the current density above $712\,\mathrm{A\,cm^{-2}}$, an output power of about 6.8 mW is achieved at 35 K. According to the cooling capacity of the cryocooler, QCL C cannot be stably operated over the whole dynamic range. For example, QCL C exhibits stable operation at 50 K for current densities up to $556\,\mathrm{A\,cm^{-2}}$ with a P_{pump} smaller

than 3.4 W. The current range for stable operation is indicated by thick lines in figure 4(a). Nevertheless, the corresponding current tuning range approaches 5.8 GHz, and the maximum output power reaches 3.6 mW in the reduced dynamic range required for stable operation so that the QCL is well suited for high-resolution absorption spectroscopy. In the temperature range between 45 and 55 K, this QCL emits a single mode, which can be tuned from -6.8 to $+3.2$ GHz with respect to the transition at 4.7448 THz.

Finally, the smooth *L–J–V* curves shown in figures 2–4 demonstrate stable, single-mode cw operation of the three QCLs (A, B, and C) over their entire tuning ranges, which is an important requirement for the acquisition of high-resolution absorption spectra. These QCLs may be used as radiation sources in THz spectrometers for the detection of absolute densities of Al atoms, N^+ ions, and O atoms in plasmas.

5. Conclusion

We have demonstrated QCLs based on GaAs/AlAs heterostructures emitting at the frequencies 3.360, 3.921, and 4.745 THz for the detection of fine-structure transitions of Al atoms, N^+ ions, and O atoms, respectively. Owing to the small electrical pump power of only a few watts, these THz QCLs exhibit stable cw operation in mechanical cryocoolers. Their dynamic ranges are sufficiently large for the evaluation of the spectral profiles of the respective absorption features. These Fabry–Pérot lasers based on single-plasmon waveguides exhibit single-mode operation with tuning ranges of more than 5 GHz and output powers of several mW. These QCLs are suitable radiation sources, which can be used for high-resolution spectroscopy to measure the absolute densities of Al atoms, N^+ ions, and O atoms in plasmas.

Data availability statement

The data that support the findings of this study are available upon reasonable request from the authors.

Acknowledgments

ORCID iDs

X Lü https://orcid.org/0000-0001-7169-7771
B Röben https://orcid.org/0000-0003-4356-5741
K Biermann https://orcid.org/0000-0003-4804-0784
J R Wubs https://orcid.org/0000-0003-2035-9099
K-D Weltmann https://orcid.org/0000-0002-4161-205X
J H van Helden https://orcid.org/0000-0001-8925-2607
L Schrottke https://orcid.org/0000-0002-0910-9163
H T Grahn https://orcid.org/0000-0001-5451-3950

References

[1] Faist J, Capasso F, Sivco D L, Sirtori C, Hutchinson A L and Cho A Y 1994 *Science* **264** 553–6
[2] Köhler R, Tredicucci A, Beltram F, Beere H E, Linfield E H, Davies A G, Ritchie D A, Iotti R C and Rossi F 2002 *Nature* **417** 156–9
[3] Williams B S 2007 *Nat. Photon.* **1** 517–25
[4] Scalari G, Walther C, Fischer M, Terazzi R, Beere H, Ritchie D and Faist J 2009 *Laser Photonics Rev.* **3** 45–66
[5] Sirtori C, Kruck P, Barbieri S, Collot P, Nagle J, Beck M, Faist J and Oesterle U 1998 *Appl. Phys. Lett.* **73** 3486–8
[6] Hübers H W, Pavlov S G, Richter H, Semenov A D, Mahler L, Tredicucci A, Beere H E and Ritchie D A 2006 *Appl. Phys. Lett.* **89** 061115
[7] Hübers H W, Richter H and Wienold M 2019 *J. Appl. Phys.* **125** 151401
[8] Alam T, Wienold M, Lü X, Biermann K, Schrottke L, Grahn H T and Hübers H W 2019 *Opt. Express* **27** 5420–32
[9] Brown J M and Evenson K M 1999 *Phys. Rev.* A **60** 956–61
[10] Chance K, Traub W A, Johnson D G, Jucks K W, Ciarpallini P, Stachnik R A, Salawitch R J and Michelsen H A 1996 *J. Geophys. Res. Atmos.* **101** 9031–43
[11] Brown J M, Varberg T D, Evenson K M and Cooksy A L 1994 *Astrophys. J.* **428** L37–L40
[12] Zink L R, Evenson K M, Matsushima F, Nelis T and Robinson R L 1991 *Astrophys. J.* **371** L85–L86
[13] Han Y J *et al* 2017 Development of terahertz frequency quantum cascade lasers for the applications as local oscillators *THz for CBRN and Explosives Detection and Diagnosis* ed M F Pereira and O Shulika (Dordrecht: Springer) pp 123–34
[14] Boreiko R T and Betz A L 1996 *Astrophys. J.* **464** L83–L86
[15] Richter H, Buchbender C, Güsten R, Higgins R, Klein B, Stutzki J, Wiesemeyer H and Hübers H W 2021 *Commun. Earth Environ.* **2** 19
[16] Hübers H W, Pavlov S G, Semenov A D, Köhler R, Mahler L, Tredicucci A, Beere H E, Ritchie D A and Linfield E H 2005 *Opt. Express* **13** 5890–6
[17] Röpcke J, Davies P B, Lang N, Rousseau A and Welzel S 2012 *J. Phys. D: Appl. Phys.* **45** 423001
[18] Röpcke J, Davies P, Hamann S, Hannemann M, Lang N and van Helden J H 2016 *Photonics* **3** 45
[19] Schrottke L *et al* 2020 *IEEE Trans. Terahertz Sci. Technol.* **10** 133–40
[20] Williams B S, Callebaut H, Kumar S, Hu Q and Reno J L 2003 *Appl. Phys. Lett.* **82** 1015–7
[21] Kloosterman J L, Hayton D J, Ren Y, Kao T Y, Hovenier J N, Gao J R, Klapwijk T M, Hu Q, Walker C K and Reno J L 2013 *Appl. Phys. Lett.* **102** 011123
[22] Bosco L, Bonzon C, Ohtani K, Justen M, Beck M and Faist J 2016 *Appl. Phys. Lett.* **109** 201103
[23] Khalatpour A, Reno J L, Kherani N P and Hu Q 2017 *Nat. Photon.* **11** 555–9
[24] Khalatpour A, Paulsen A K, Addamane S J, Deimert C, Reno J L, Wasilewski Z R and Hu Q 2022 *IEEE Trans. Terahertz Sci. Technol.* **12** 144–50
[25] Schrottke L, Wienold M, Sharma R, Lü X, Biermann K, Hey R, Tahraoui A, Richter H, Hübers H W and Grahn H T 2013 *Semicond. Sci. Technol.* **28** 035011
[26] Wienold M, Röben B, Schrottke L, Sharma R, Tahraoui A, Biermann K and Grahn H T 2014 *Opt. Express* **22** 3334–48
[27] Heyminck S, Graf U U, Güsten R, Stutzki J, Hübers H W and Hartogh P 2012 *Astron. Astrophys.* **542** L1
[28] Richter H, Wienold M, Schrottke L, Biermann K, Grahn H T and Hübers H W 2015 *IEEE Trans. Terahertz Sci. Technol.* **5** 539–45
[29] Rezac L, Hartogh P, Güsten R, Wiesemeyer H, Hübers H W, Jarchow C, Richter H, Klein B and Honingh N 2015 *Astron. Astrophys.* **580** L10
[30] Hagelschuer T, Richter H, Wienold M, Lü X, Röben B, Schrottke L, Biermann K, Grahn H T and Hübers H W 2019 *IEEE Trans. Terahertz Sci. Technol.* **9** 606–12
[31] Lü X, Röben B, Schrottke L, Biermann K and Grahn H T 2021 *Semicond. Sci. Technol.* **36** 035012
[32] Röben B, Lü X, Biermann K, Schrottke L and Grahn H T 2019 *J. Appl. Phys.* **125** 151613
[33] Schrottke L, Lü X, Rozas G, Biermann K and Grahn H T 2016 *Appl. Phys. Lett.* **108** 102102
[34] Biermann K, Helgers P L J, Crespo-Poveda A, Kuznetsov A S, Röben B, Lü X, Schrottke L, Santos P V and Grahn H T 2021 *J. Cryst. Growth* **557** 125993